

# What you thought you already knew about the bending motion of triatomic molecules

Wolfgang Quapp

*Mathematisches Institut, Universität Leipzig, D-04109 Leipzig, Germany*

Brenda P. Winnewisser

*Physikalisch-Chemisches Institut, Justus-Liebig-Universität,  
D-35392 Gießen, Germany*

Received 4 June 1992; revised 1 October 1992

The bending vibrations of linear, quasilinear, and bent molecules are qualitatively different phenomena. Each of these cases has been fully described by quantum mechanical formulations in the last half century, but important two-dimensional aspects of all three cases as well as the relationship between the three types of bending behavior remain difficult to visualize. Simple two-dimensional figures can help to provide an introduction to basic spatial and mathematical aspects of the bending problem.

## 1. Introduction

We have found that chemists, physicists and mathematicians frequently have conceptual difficulties when first confronted with the subject of the dynamics of the bending of triatomic molecules. The present treatment is the result of our efforts to deal with the hidden assumptions and frequent misconceptions associated with this apparently simple problem; a subject in molecular physics which is, in principle, mathematically solved.

In the bending vibration of a triatomic molecule, the balance of contributions to the electronic energy may define a potential energy surface (PES) for a given electronic state in which the potential minimum describes a linear configuration (e.g., HCN, ground state) or a bent configuration (e.g., HCN,  $^1A''$  states). Quantum mechanical methods for calculating PES [1], energy levels and eigenfunctions [2] over the full range between these limiting cases have been available for some years with varying degrees of rigorousness [3–10]. The present contribution seeks to emphasize, with a graphical representation of the eigenfunctions, some of the properties of these wave functions, and the eigenstates they describe, over the full range of potential surfaces of triatomic molecules.

Let us look first briefly at the properties of the PES. For a molecule in the linear configuration, viewed in the space defined by a Cartesian molecule-fixed coordinate system, of which one axis coincides with the linear equilibrium configuration, all directions of a possible bending distortion have the same weight. Thus, the PES is isotropic in two dimensions (2D). If the equilibrium position is not the linear configuration, there is a potential hump, or a barrier, at the linear configuration. Definitions have been introduced to describe mathematically the range of possible molecular PES of polyatomic molecules [3]. In the framework of these definitions, a barrier at the linear configuration is classified as "a proper saddle point of the PES of index 2," surrounded by a circular minimum [3]. Index 2 means that the Hessian matrix, the matrix of second partial derivatives with respect to the coordinates of the PES, has two negative eigenvalues. This property is seen in applying a normal coordinate analysis to a PES derived, for example, from *ab initio* or semiempirical molecular orbital calculations. Evaluation of the Hessian matrix at the equilibrium configuration of the molecule yields the force constants, but at the saddle point of index 2 it yields 2 negative force constants, which lead to imaginary normal frequencies.

If the barrier to linearity is very high, we say the molecule is bent. In this case, we shift our evaluation of the Hessian matrix to the configuration at the minimum of the PES to obtain a physically meaningful vibrational force constant.

If the barrier height is comparable to the energies of the lowest levels of the bending mode, we classify a molecule as quasilinear [4]. This means, among other things, that the Hessian matrix at neither the linear configuration nor the configuration of the minimum yields values that can be simply related to the bending energy intervals. The story of the study of the anomalous spectra associated with triatomic quasilinearity goes back to Thorson and Nakagawa [11].

For this study, we now choose a coordinate system which allows us to display the two dimensions relevant to the bending motion for all of these cases. A molecule-fixed coordinate system is defined as usual by using the Eckart conditions [12]. This allows us to separate off the three translational degrees of freedom and to define a reference configuration, relative to which there is no rotation but only vibration. Finally we determine the principal axes of inertia of the reference configuration, which are then the molecule-fixed  $a$ ,  $b$ , and  $c$  axes. We can then define the three Euler angles  $\theta$ ,  $\chi$ , and  $\phi$  describing the rotation of this molecule-fixed axis system relative to the space-fixed axes. In the case of a bent reference configuration, the third Euler angle,  $\phi$ , describes the rotation of the molecule about the molecule-fixed  $z$  or  $a$  axis. In the case of a linear reference configuration, this angle is undefined. It has meaning only for describing the phase of the degenerate bending motion, as will be seen below. We will write the Hamiltonian for the three-atom molecule in terms of these conventional molecule-fixed axes, but will present the graphic material in all cases in the Cartesian coordinate system in which the  $x$  axis corresponds to  $\phi = 0$ . Thus, we show the properties of the system in the  $xy$  plane, which is shown in fig. 1. Although this axis system corresponds to the conventional

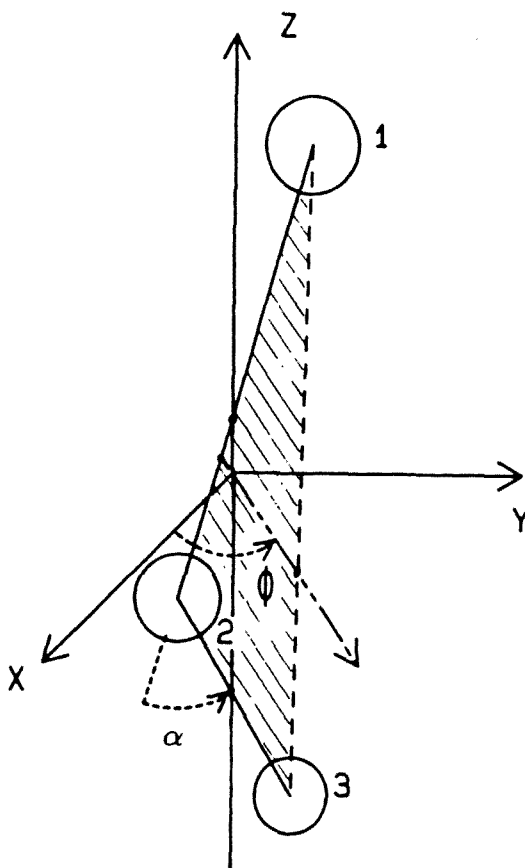


Fig. 1. Coordinates  $\phi$  and  $\alpha$  employed in the description of linear and nonlinear molecules. Atoms are designated by the labels 1 to 3. The  $x, y$  coordinates of atom 2 are negative in the given configuration.  $z = a$  is the molecule-fixed axis of least moment of inertia, and the Euler angle  $\phi$  describes the rotation of the molecular plane 123 around  $z$ .  $\alpha$  describes the molecular bending in the plane 123.

molecule-fixed axis system for the linear case, it is only “partially molecule-fixed” for the bent case.

If we choose displacement coordinates relative to the reference configuration, for which the potential  $V$  is a minimum and transform to normal coordinates  $Q_i$ , then the kinetic energy  $T$  has no cross terms between vibrational coordinates, in the harmonic approximation, and the reduced mass for each vibrational coordinate is a constant. We shall ignore the role of stretching motions. We are concerned only with the bending motion described by a displacement in the angle  $\alpha$ , which is the bond angle supplement of the molecule, shown in fig. 1. If the reference configuration is linear, then the displacement is equal to the value of  $\alpha$  itself. We can thus represent any bending of a triatomic molecule and any rotation around the figure

axis by the two coordinates  $(\alpha, \phi)$ . It should be noted, however, that this representation is not suitable for the class of triatomic molecules which exhibit internal rotation, and this class of molecules is not treated here.

The Hamiltonian for the dynamics of the isolated three-atomic molecule can thus be represented schematically in a first approximation as [4]

$$\mathbf{H} = \underbrace{\{T_s + V_s\}}_{\text{ignored}} + \underbrace{\{T_b + V_b + T_{R(A)}\}}_{\text{studied here}} + \underbrace{\{T_{R(B,C)}\}}_{\text{ignored}}, \quad (1)$$

where the first bracket represents the stretching motion, the central bracket represents the bending and rotation motion, described by the two coordinates  $\alpha$  and  $\phi$  shown in fig. 1, and the last term gives the end-over-end rotation.  $T$  is the kinetic energy and  $V$  the potential energy associated with each type of motion.  $T_{R(A)}$  and  $T_{R(B,C)}$  refer to the kinetic energy of rotation about the  $a$ ,  $b$  and  $c$  axes in the bent molecule. The first and last brackets (and thus stretch-bend and end-over-end-rotation-stretch interactions) will be omitted in the following treatment, since only the central part of eq. (1) is of interest in this paper ("rigid bender" approximation [5]).

In section 2 we review the conventional treatment of the linear harmonic molecule, and we consider the 2D aspects of both classical and quantum-mechanical perspectives, including in section 2.4 the implications of the definition of the volume element in the quantum mechanical description. In section 3 we consider anharmonic oscillators, in section 4 quasilinear molecules, and in section 5 bent triatomics. Although the limiting case of a bent molecule is more familiar, we will treat first the quasilinear molecule which follows logically the discussion of anharmonic linear models. Finally, there follows a brief discussion of extensions to more complex PES geometries.

## 2. The linear case

### 2.1. THE CLASSICAL EQUATIONS OF MOTION

A bending displacement from the linear configuration,  $\alpha$  in fig. 1, can occur in any direction of the  $xy$  plane. If it is of small amplitude, it can be described by a combination of two orthogonal rectilinear displacement coordinates,  $Q_x$  and  $Q_y$ . The normal coordinate  $Q_x$  represents a displacement  $\delta x_i$  of each atom fulfilling the Eckart conditions. The distortion of the molecule constitutes an oscillator. We wish to evaluate the potential and kinetic energies of this oscillator. The potential energy in the two displacement coordinates  $Q_x$  and  $Q_y$  is an isotropic surface which in the harmonic approximation is a paraboloid. The oscillator itself may be represented by a particle of reduced mass  $\mu$  moving in the  $Q_x Q_y$  plane subject to a linear

restoring force directed towards the coordinate origin. The equations of motion are

$$\mu\ddot{Q}_x = -\lambda Q_x \quad \text{and} \quad \mu\ddot{Q}_y = -\lambda Q_y, \quad (2)$$

where  $\ddot{Q}$  is the second derivative with respect to time and  $\lambda$  is the force constant. The energy is given in classical Hamiltonian form by

$$\mathbf{H} = \frac{1}{2\mu} (P_x^2 + P_y^2) + \frac{\lambda}{2} (Q_x^2 + Q_y^2), \quad (3)$$

where the linear momenta are  $P_j = \partial T / \partial \dot{Q}_j$ ,  $j = x, y$ , where  $T$  is the kinetic energy. We set

$$2\pi\omega = (\lambda/\mu)^{1/2} \quad (4)$$

and obtain

$$\mathbf{H} = \frac{1}{2\mu} (P_x^2 + P_y^2) + 2\mu(\pi\omega)^2 (Q_x^2 + Q_y^2). \quad (5)$$

The transformation to dimensionless coordinates and linear momenta

$$q_i = (2\pi\mu\omega/\hbar)^{1/2} Q_i, \quad p_i = (1/\mu\omega\hbar)^{1/2} P_i \quad (6)$$

brings the classical Hamiltonian  $\mathbf{H}$  to the form

$$\mathbf{H} = \frac{1}{2}\hbar\omega\{(p_x^2 + p_y^2) + (q_x^2 + q_y^2)\} = \mathbf{T} + \mathbf{V}. \quad (7)$$

## 2.2. THE QUANTUM MECHANICAL EQUATIONS OF MOTION AND THEIR SOLUTIONS

The Schrödinger equation is derived by using the relation  $p_j = -i\partial/\partial q_j$  for the linear momenta, giving

$$-\left(\frac{\partial^2\psi}{\partial q_x^2} + \frac{\partial^2\psi}{\partial q_y^2}\right) + (q_x^2 + q_y^2)\psi = \left(\frac{2E}{\hbar\omega}\right)\psi, \quad (8)$$

with the wave function  $\psi(q_x, q_y)$  and eigenvalue  $E$ . We can introduce planar polar coordinates, a dimensionless bending amplitude  $r$  and the Euler angle  $\phi$ , by writing  $q_x = r \cos \phi$  and  $q_y = r \sin \phi$ , where  $r \geq 0$  and  $0 \leq \phi < 2\pi$ . Note that  $r$  approximates  $\alpha$  near zero. Equation (8) transforms into

$$\left\{ \left( \frac{\partial^2}{\partial r^2} + \frac{1}{r} \frac{\partial}{\partial r} + \frac{1}{r^2} \frac{\partial^2}{\partial \phi^2} \right) + \left( \frac{2E}{\hbar\omega} - r^2 \right) \right\} \psi(r, \phi) = 0. \quad (9)$$

With the function  $\psi(r, \phi) = \psi(r) \exp(i\ell\phi)$  we have the well-known solution which allows the separation of the wave functions for bending and angular motion. Since  $\exp(i\ell\phi) = \cos(\ell\phi) + i \sin(\ell\phi)$ , we see that for arbitrary values of  $\ell$  this function is

not single-valued for the same point in space  $\phi = 0$  and  $\phi = 2\pi$ . Hence,  $l$  has to be an integer. Inserting the  $\exp(il\phi)$  solution we can integrate over the variable  $\phi$  in eq. (9) and obtain

$$\left\{ \left( \frac{\partial^2}{\partial r^2} + \frac{1}{r} \frac{\partial}{\partial r} \right) + \left( \frac{2E}{\hbar\omega} - r^2 - \frac{l^2}{r^2} \right) \right\} \psi_l(r) = 0. \quad (10)$$

This is the standard form of an isotropic 2D oscillator. The problem is reduced, for any given integer value of the quantum number  $l$ , to a one-dimensional Schrödinger equation with an extended potential containing the value of  $l$ . The bending vibration is thus necessarily coupled to a rotation about the linear axis, which correlates with the  $a$  axis, the principal axis of least moment of inertia of a bent molecule.  $V(r) = (\hbar\omega/2)r^2$  is replaced by the "effective" potential

$$V_{\text{eff}}(r) = \frac{\hbar\omega}{2}(r^2 + l^2/r^2). \quad (11)$$

In fig. 3 we illustrate the two parts ( $r^2$  and  $l^2/r^2$ ) of  $V_{\text{eff}}$  and their combination. The dramatic difference in the slopes for  $r \rightarrow 0$  comes from the singular term and it leads to a bending wave function  $\psi_l(r)$  which is quite different from the analogs of eq. (8) in the case of a 1D harmonic oscillator. The solution of eq. (10) leads to eigenfunctions which are given by

$$\psi_{n,l}(r) = N_{n,l} \exp(-r^2/2) r^l L_{n+l}^l(r^2), \quad l \geq 0, \quad (12)$$

with

$n$  = quantum number of bending amplitude,  $n = 0, 1, 2, \dots$ ,

$l$  = quantum number of angular motion,  $l = v, v-2, v-4, \dots, -v$

(if  $l < 0$  we use  $|l|$  in formula (12)),

$v = 2n + |l| = 0, 1, 2, \dots$  overall bending quantum number of the state,

$N_{n,l}$  = factor for normalization =  $(n!/\{(n+l)!\}^3 \pi)^{1/2}$

and

$$L_{n+l}^l(r^2) = [(n+l)!]^2 \sum_{m=0}^n (-r^2)^m / [m!(n-m)!(l+m)!] \quad (13)$$

is the associated Laguerre polynomial [13,14] of degree  $(r^2)^n$ .

The eigenfunctions for  $|l| > 0$  all have the property of being zero when  $r$  is zero. The explicit form of  $\psi(r)$  and its behavior at  $r = 0$ , for all  $l$ , depends on the representation of the volume element used explicitly or implicitly for the integration of the Schrödinger equation. This choice is discussed in detail below in section 2.4.

The energy eigenvalue of state  $v$  is

$$E_v = \hbar\omega(v+1) = \hbar\omega(2n + |l| + 1), \quad (14)$$

which stipulates that the state  $v$  is  $(v+1)$ -fold degenerate in the case of a harmonic potential [15], since we can combine  $(v+1)$  different values of  $2n$  and  $l$  which yield the same  $v$  and  $E_v$ . However, the usual statement " $E_v$  is independent of  $l$ " [2] is

not the full truth! It is important to remember that even though the energy, in a first approximation, is described by  $v$ , the real quantum numbers are  $n$  and  $l$ . In spectroscopy, the quantum numbers  $(v, l)$  are used in the linear limit, yet the bending amplitude quantum number  $n$  usually is not. In fig. 2 we have drawn the levels  $v = 0, \dots, 4$ . If we treat as an example the case  $v = 4$ , we have to take into account the pair of combinations  $(n = 2, l = 0)$ ,  $(n = 1, |l| = 2)$ , and  $(n = 0, |l| = 4)$ . *It follows that very different dynamic states of a molecule give the same eigenvalue.*

### 2.3. THE CLASSICAL TRAJECTORIES OF THE LINEAR MOLECULE BENDING

The classical representation of the 2D oscillator representing a linear molecule bending, mapped in the oscillator space of  $q_x$  and  $q_y$ , takes the form of the ellipses shown in fig. 4. This figure shows the classical trajectories of the oscillator corresponding to various combinations of  $l$  and  $n$  possible for  $v = 4$ , in a classical picture. If  $l = v$ , the trajectories in fig. 4 are circles. There is thus no bending motion, or change in  $r$ . The motion of the molecule is actually a pure rotation of the plane of the molecule about the  $z$  axis.

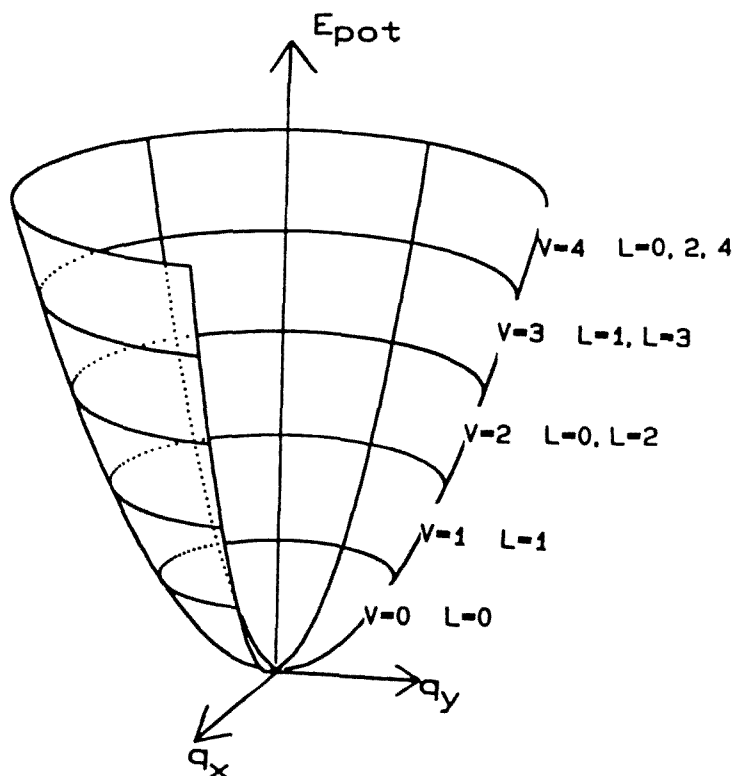


Fig. 2. The 2D isotropic harmonic oscillator: model PES for the bending vibration of a linear molecule. The outer wall is opened for better insight.

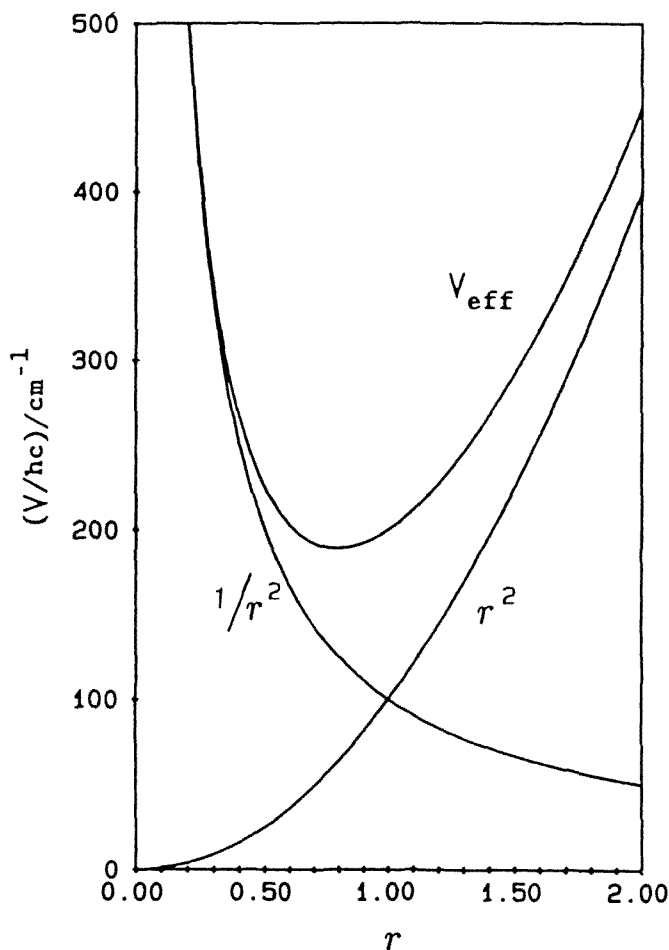


Fig. 3. The effective potential  $V_{\text{eff}}$  of a typical triatomic molecule for  $l \neq 0$  and its component parts, the purely bending function  $r^2$ , and the angular contribution  $l^2/r^2$  in the case of  $l = 1$ .

The corresponding movement of a triatomic molecule in the space of fig. 1 is sketched in fig. 5, in two snapshots at different times. This apparently simple conclusion is represented incorrectly in established texts. There are basic errors in Goldstein's representation [16], and an incorrect implicit phase in Atkins' figure [17]. The atoms follow a path around the axis of the least moment of inertia, and the circles representing the trajectories in the case of pure rotation are more or less flattened into ellipses by the amplitude of the radial bending coordinate [18]. The ellipses maintain a fixed ratio of major to minor axes in both pictures. The relative contributions of the angular energy and of the bending amplitude energy determines the difference between the major and minor axes. If  $l = 0$  then a pure bending vibration takes place, and the ellipse degenerates into a trajectory along a straight line passing through the linear configuration. If the kinetic energy is entirely centri-



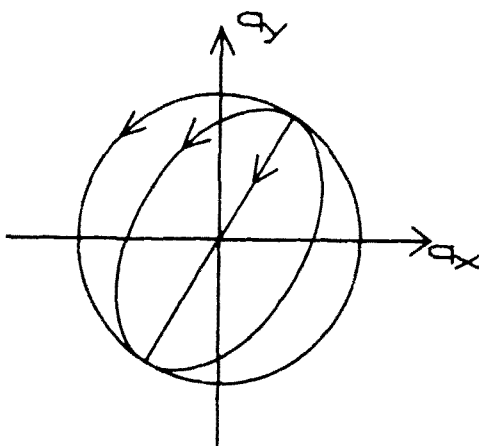


Fig. 4. Classical picture of the trajectories of combined bending-angular movement in a linear molecule in the excited degenerate vibrational state with  $v = 4$ . The straight arrow through the origin depicts a pure bending vibration ( $n = 2, l = 0$ ), the ellipse a combined bending-rotation motion ( $n = 1, l = 2$ ), and the circle a pure rotation ( $n = 0, l = 4$ ).

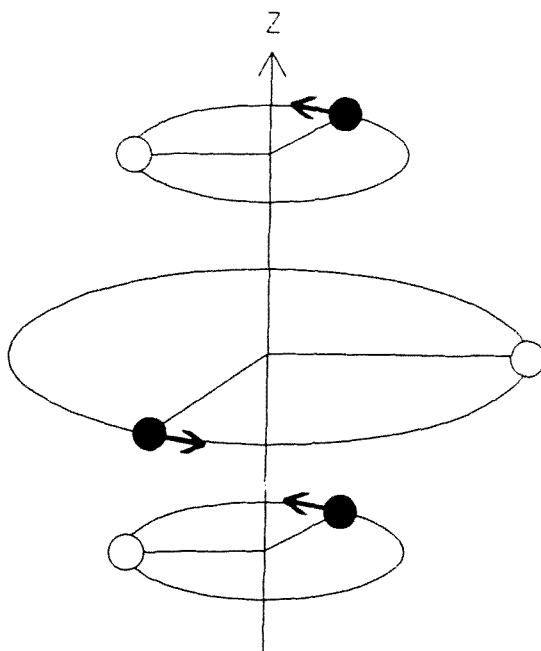


Fig. 5. Classical bending and rotation trajectory in the  $x, y$  plane of a linear symmetric triatomic in a direct view. Note that we can have actually ellipses for  $n > 0, l < v$ , not only in the perspective view of the picture.

fugal energy, that is when  $l = v$ , the trajectory is a circle equivalent to a pure rotation of the molecule. For intermediate values of  $l$  the figure will be an ellipse lying between these two limiting extremes.

#### 2.4. THE VOLUME ELEMENT FOR THE INTEGRATION OF THE SCHRÖDINGER EQUATION

The wave functions and their graphical representation depend in an important manner on the (2D) volume element defined for the integration over the wave functions [19]. The planar polar coordinates that are so suitable for setting up the wave functions and carrying out quantitative calculations have the property of being curvilinear in the  $q_x, q_y$  plane and show special behavior at  $r = 0$ . Whereas we would write the probability distribution in Cartesian coordinates as  $|\psi(q_x, q_y)|^2 dq_x dq_y$ , we must write it in polar coordinates as  $|\psi(r, \phi)|^2 r dr d\phi$ . The  $\phi$  contribution in the square of the wave function,  $|\exp(i l \phi)|^2$ , is equal to one for all values of  $\phi$ , and  $d\phi$  is constant over  $\phi$ . However,  $r dr$  is not constant over the range of  $r$ : the area of every annular element around the point  $r = 0$  becomes greater as  $r$  increases. This is shown in fig. 6, where the Cartesian coordinate perspective and the polar coordinate perspective are both superimposed on a PES. When the quantity

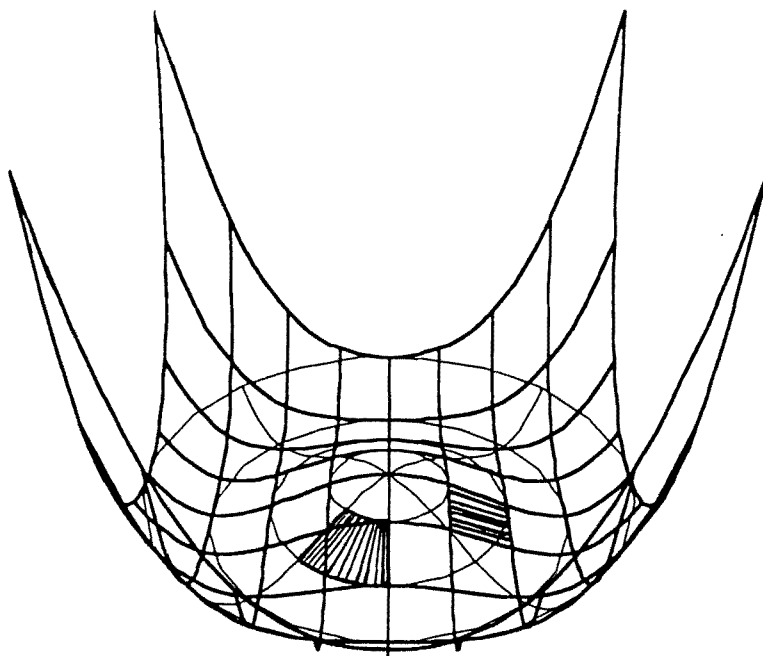


Fig. 6. Model PES drawn with two grids, one defined by Cartesian coordinates  $q_x$  and  $q_y$  and one defined by the corresponding polar coordinates. The radial coordinate is  $\alpha$ , and the coordinate of rotation of the figure is  $\phi$ . The difference shows up in the behavior of the volume elements derived from the two grids.

$$|\psi(r, \phi)|^2 r dr = |\sqrt{r}\psi(r, \phi)|^2 dr = |\psi_r(r)|^2 dr$$

is plotted against the linear  $r$  axis, then its amplitude goes to zero at  $r = 0$ , even for  $l = 0$ . This  $\psi_r(r)$  on the right side is the wave function used, and obtained numerically, throughout the theory of rigid and nonrigid bender Hamiltonians [5,6]. Since the volume element at  $r = 0$  has zero area, it can be legitimately argued that the probability (even for a "linear" molecule) of finding the molecule in the volume element corresponding to the linear configuration,  $2\pi\delta r$  at  $r = 0$ , is actually zero. Furthermore, in the quantum-mechanical picture we cannot discuss the probability of the molecule "passing through" any given configuration, since the concept of a sequential trajectory has been left behind with classical mechanics. In order to make this change in perspective less abrupt, we can divide out the factor  $r$ , and look at the amplitude of  $|\psi(r)|^2 = |\psi_r(r)/\sqrt{r}|^2$  as a function of  $r$ . We then obtain the probability distribution corresponding to the "Cartesian perspective" shown in fig. 6 and implicit in some other studies [20]. The two wave functions,  $\psi_r(r)$  and  $\psi(r)$ , are shown in fig. 7 for a harmonic potential [6,21,22].

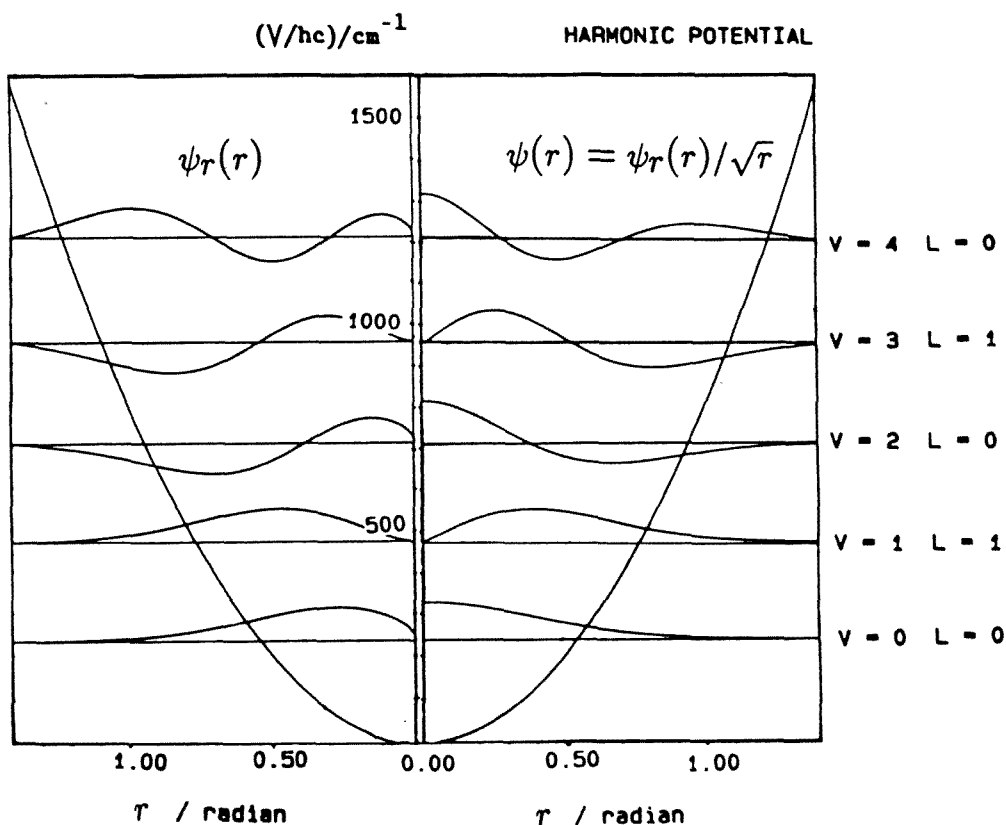


Fig. 7. Wave functions in a parabolic model potential  $ar^2$  with coefficient  $a = 800 \text{ cm}^{-1}$ , giving a 1D-resumé of the problem of the 2D isotropic oscillator: (left)  $\psi_r(r)$  for which the value of the function at  $r = 0$  is always zero; (right) wave functions  $\psi(r) = \psi_r(r)/\sqrt{r}$ .

The two-dimensional diagrams of wave functions in this presentation show consistently the wave function  $\psi(r)$ . However, we should not lose sight of the fact that only one parameter,  $r$ , contains information about the restoring force, and that the probability density, since it is the square of the complex wave function, cannot depend on  $\phi$ . Thus, for quantitative calculations of observable quantities the wave function  $\psi_r(r)$  and its volume element  $dr$  are entirely appropriate.

## 2.5. THE WAVE FUNCTIONS

From this point we will maintain the quantum-mechanical perspective. In fig. 8 we see the real part of the bending wave functions of eq. (12) in a 2D harmonic bending potential for  $v = 0$  and  $v^l = 4^0, 4^2$ , and  $4^4$ . The wave functions for  $l = 0$  have full rotational symmetry about the center. But for quantum numbers  $l = 2$  or  $4$ , we obtain an influence of  $l$  in the form of a rotational variation around the center. The wave seems to oscillate about the center, which itself is a forbidden point; as noted above, all eigenfunctions for  $|l| > 0$  are zero for  $r = 0$ . This means that the probability of the molecule being found in the linear configuration is zero [24]. Linear molecules with  $l > 0$  do not carry out a "pure" bending vibration because their nuclei orbit about the axis of linearity. The effective potential contains an angular momentum barrier at linearity, which means that the probability density is only significant for a centrifugally bent configuration, represented classically in figs. 4 and 5.

There is a difficulty in visualizing the dynamics of the molecule that lies in the different mathematical language of description in quantum mechanics and classical mechanics: for example, pure rotation described classically to be on a circle of fixed radius  $r$  in the  $q_x q_y$  plane must be expressed in quantum mechanics by a wave function  $\psi_{0,l}$ , ( $n = 0, l = v$ ) which gives a probability distribution  $|\psi_{0,l}|^2$  over an extended range of radii  $r$ . Indeed, rather than visualizing the dynamics, in the sense of following a trajectory, we must learn to visualize the probability density.

Similarly, a pure 1D, straight classical trajectory of the vibration  $v = 2n, l = 0$ , along a fixed  $\phi$  direction is in the quantum-mechanical picture an intrinsically 2D vibration, where the bending wave function  $\psi_{n,0}$  is centrally symmetrical and thus distributed uniformly over all values of  $\phi$ . Described in terms of Cartesian displacements, both of the coordinate directions,  $q_x$  and  $q_y$ , are equally excited with quantum number  $n$ , and with the same phase. Thus, because we have a 2D isotropy, for such states only even values of  $v$  are possible. In the case  $l \neq 0$  with any value of  $n$  we see the variable  $\phi$  as a cyclic variable. However, the value of  $\phi$  and thus the wobbles in amplitude around the linear configuration due to the factor  $\exp(il\phi)$  in  $\psi_{n,l}$  are ultimately ignorable in an isolated molecule, since the probability density distribution is given by the square of the wave function over the range of a rotation  $0 < \phi < 2\pi$ . Thus, the classical 2D problem in  $(r, \phi)$  transforms to a 2D wave function but this reduces to a 1D representation of the probability distribution along the bending coordinate  $r$ . The angle  $\phi$  is an Euler angle, but the above discussion

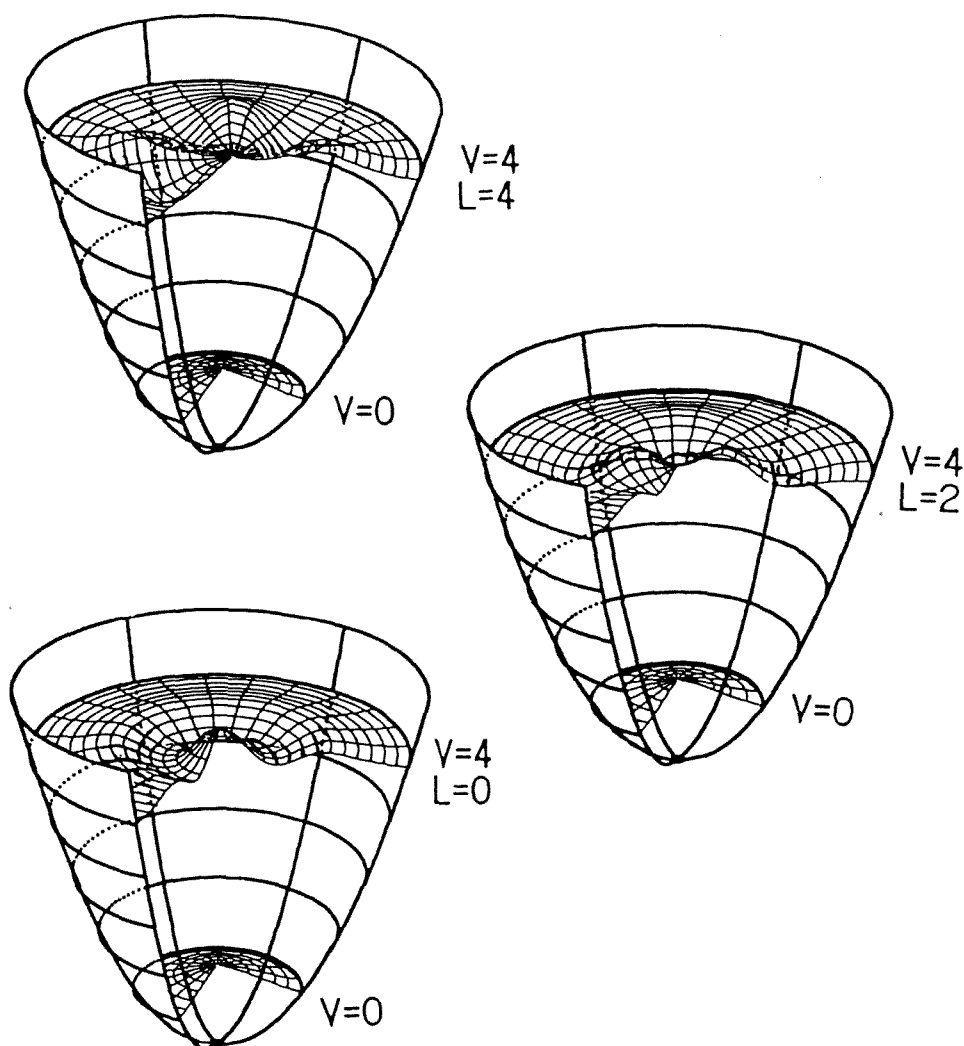


Fig. 8. Real part of the wave functions for  $v = 0$  and  $v = 4^l$  of a linear molecule with  $l = 0, 2, 4$ . The radial coordinate is  $\alpha$ , and the coordinate of rotation of the figure is  $\phi$ . The plots are made using procedures of ref. [23].

shows that in a linear molecule, it corresponds to an arbitrary phase factor [25]. This phase information will only play a role in observable quantities when the isotropy is perturbed, as in collisional processes.

The physical meaning of the wobbles in amplitude of the real part, for example, of the wave functions with  $l > 0$  in fig. 8, is the following: the number of nodes between  $0$  and  $\pi$  gives the quantum number  $l$ . This  $l$  has its origin in a derivative of

the wave function with respect to  $\phi$ , which represents the angular momentum operator,  $-i\hbar\partial/\partial\phi = (q_x p_y - q_y p_x)$ , so that  $l\hbar$  is the angular momentum eigenvalue. Thus, even though the probability distribution is uniform in  $\phi$ , the rotational excitation is described by the oscillations of the wave function which, when the time coordinate  $t$  is added, are seen to rotate around the center.

Any departure from the harmonic approximation results in a lifting of the degeneracy of states for a given  $v$  which display such different forms of behavior. Indeed, even for a purely harmonic PES, a slight lifting of the degeneracy results from the spatial extent of a real molecule when the curvilinear coordinate  $\alpha$  is used and the angle dependence of the reduced mass is not neglected; i.e., when a rigorous representation of the kinetic energy of a real molecule is employed [21]. (In the above derivation, as in all introductory treatments of molecular vibrations, we have approximated the curvilinear bending vibration by rectilinear normal coordinates  $q_i$  with a constant reduced mass.) In a model molecule with the masses and internuclear distances of HCNO, in a parabolic potential like in fig. 7 and treated as a rigid bender with a curvilinear angular coordinate for the HCN-bending vibration, there results for  $v = 4$  a downward shift of energy with increasing  $l$ , such that one finds a difference of  $5 \text{ cm}^{-1}$  between the lowest state ( $n = 0, l = 4$ ) and the state ( $n = 2, l = 0$ ) in a harmonic potential  $a\alpha^2$  with  $a = 800 \text{ cm}^{-1}$ , i.e. a difference of 0.6% of one vibrational quantum.

When the rotational energy, the last term in eq. (1), is also considered, there is a twofold degeneracy of each level with  $l > 0$  which is lifted by so-called  $l$ -type doubling and resonance [2,26]. If we trace the ladder of end-over-end rotational states, with quantum numbers  $J \geq l$ , we find splittings and shifts of the levels. Classically, we can distinguish between different directions of vibrational angular momentum relative to the end-over-end rotational angular momentum. The quantum-mechanical waves are characterized by different parities for the two corresponding nearly degenerated states. The resulting interactions, however, are much smaller than the effects we are discussing and are mentioned here only for completeness.

### 3. The linear triatomic molecule as anharmonic oscillator

We move now to a more realistic potential energy curve  $V(r)$  or  $V(\alpha)$  than the purely harmonic potential in eqs. (3)–(11), for the bending of a triatomic molecule. In general, for real linear molecules, two cases are important. The first is a potential whose outer wall is less steep than a parabola. In the second case the potential well is steeper.

In the general case of an arbitrary bending potential  $V(\alpha)$  there is no explicit analytic solution. Therefore we must use numerical approximations. The main point of interest will be seen to be the removal of the degeneracy of  $E_v$  in  $(n, l)$  found in eq. (14).

Case (i):  $V(\alpha)$  less steep than  $\alpha^2$

An example of an anharmonic potential is the Gaussian potential function

$$V_{\text{anh}}(\alpha) = D[1 - \exp(-b\alpha^2)]. \quad (15)$$

The most extreme form of this type of potential is found in the case of an interaction of the bending mode with a weak stretching mode and describes van der Waals-molecules [14]. In a more moderate form it is also found in the largely ionically bound alkali hydroxides, KOH [27], RbOH and CsOH. Near the equilibrium position the potential is quadratic and symmetric, and can be approximated as  $Db\alpha^2$ , while at larger values of  $\alpha$  the function opens and asymptotically approaches either a dissociation limit,  $D$ , similar to that of a Morse potential, or a barrier to isomerization and internal rotation: The molecule 1-2-3 in fig. 1 becomes, as  $\alpha$  approaches  $90^\circ$ , molecule 2-3-1, which should be then represented by another potential function, but of a similar form. We retain here the angular coordinate  $\alpha$  in order to treat the more extreme cases, where  $\alpha$  is not infinitesimal. We transform  $\alpha$  using  $2Db = \lambda$  as a force constant so that with a new coordinate  $\rho$  in place of  $\alpha$  we have

$$\rho^2 = \sqrt{2Db\mu}\alpha^2/\hbar. \quad (16)$$

We can then define

$$\gamma = \hbar[b/(2D\mu)]^{1/2} \quad \text{and} \quad \omega = (2Db/\mu)^{1/2}/2\pi, \quad (17)$$

and eq. (10) becomes

$$\left\{ \frac{\partial^2}{\partial \rho^2} + \frac{1}{\rho} \frac{\partial}{\partial \rho} - \frac{l^2}{\rho^2} - \frac{1}{\gamma} [1 - \exp(-\gamma\rho^2)] + \frac{2E}{\hbar\omega} \right\} \psi_l(\rho) = 0. \quad (18)$$

A perturbation approach works well if the difference between the potential of eq. (15) and the harmonic oscillator potential  $Db\alpha^2$  is small, as is the case with small  $\gamma$  where  $D \gg b$ . Then we replace the potential term of eq. (15) with

$$V_{\text{anh}}(\rho) = \rho^2 - (\rho^2 - \frac{1}{\gamma} [1 - \exp(-\gamma\rho^2)]) = V_{\text{harm}}(\rho) - \Delta V(\rho), \quad (19)$$

and use the term  $\rho^2$  in the formulation of eq. (10) for exact basis eigenfunctions and eigenvalues. The following notation is used:

$$\begin{aligned} \mathbf{H}_{\text{harm}}\psi_{nl}(\rho) &= E_v\psi_{nl}(\rho) \quad (\text{cf. eq. (10)}), \\ \mathbf{H}_{\text{anh}}\psi_{nl}^{\text{anh}}(\rho) &= \epsilon_{nl}\psi_{nl}^{\text{anh}}(\rho), \end{aligned} \quad (20)$$

where the  $\mathbf{H}$ 's are operators,  $\psi_{nl}$  and  $\psi_{nl}^{\text{anh}}$  are eigenfunctions, and  $E_v, \epsilon_{nl}$  are eigenvalues of the  $v$ th eigenfunctions of the harmonic and anharmonic Hamiltonian operators, respectively. The anharmonic eigenfunctions  $\psi_{nl}^{\text{anh}}$  can be expanded in terms of the complete set of unperturbed harmonic eigenfunctions  $\psi_{nl}(\rho)$ . Additionally, one assumes that the eigenvalues  $\epsilon_{nl}$  can be expanded in terms of a converging series of perturbation corrections to the unperturbed (zeroth-order) energy:

$$\epsilon_{nl} = E_{nl} + \epsilon_{nl}^{(1)} + \epsilon_{nl}^{(2)} + \dots \quad (21)$$

The expansion of eq. (21) can be extended to obtain the desired degree of accuracy of the eigenvalues  $\epsilon_{nl}$ .

The resulting eigenvalues show the expected removal of degeneracy in the form of an increase in energy with  $l$  for a given  $v = (2n + l)$ . In the extreme case of a "shallow well" with  $D = 1000 \text{ cm}^{-1}$  and  $b = 1$  in eq. (15), shown in fig. 9, the splitting of these energy levels for a given  $v$  is substantial.

*Case (ii): The linear triatomic molecule as quartic anharmonic oscillator*

We now want to study anharmonicity that tends in the direction of a "hinge"

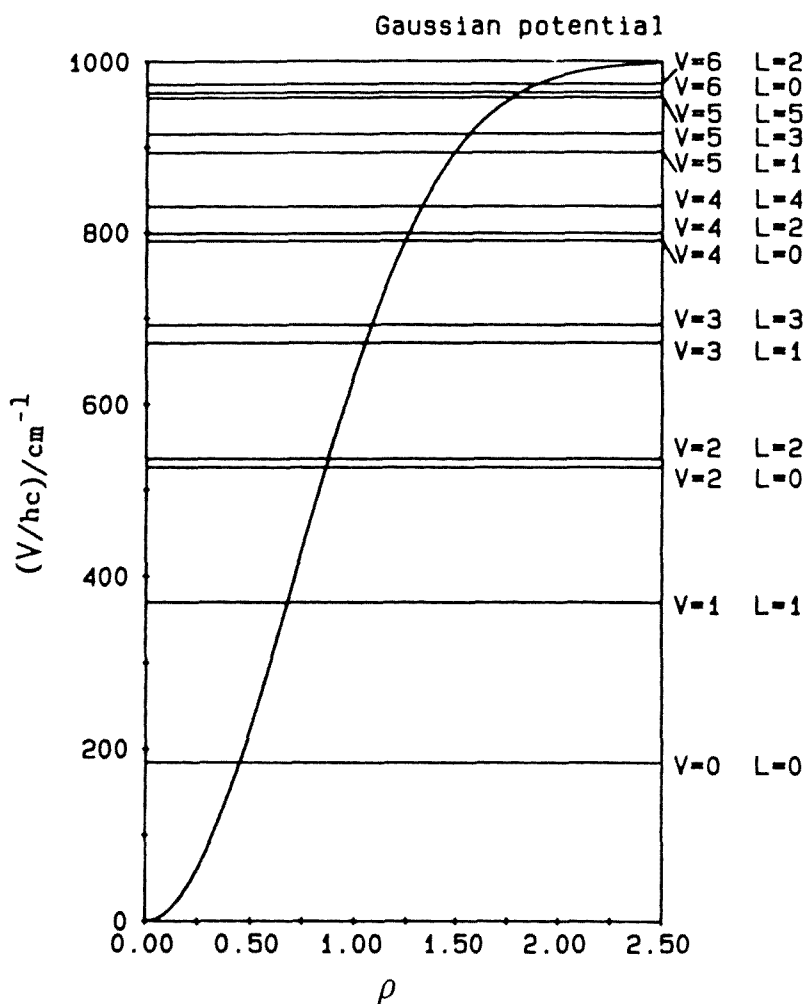


Fig. 9. 1D cut through the uniquely defined range of a Gaussian energy well with  $D = 1000 \text{ cm}^{-1}$ ,  $b = 1$ , and energy levels  $(v, l)$  given by perturbation theory. The calculated values are from Lieb et al. [14].



potential [28,29] which corresponds to a potential wall representing the repulsion of the two outer atoms when they approach each other at large bending angles. This can be described in general by a potential in  $\alpha$  steeper than quadratic, given by

$$V(\alpha) = a\alpha^2 + b\alpha^4 + \dots \quad \text{with } a, b, \dots \geq 0. \quad (22)$$

Because of symmetry, any polynomial representation of  $V$  contains even order terms only. So long as the anharmonic contribution is small, it is usually sufficient to consider only the quartic term, in addition to the dominant quadratic term. In this case, we can, as before, approximate the motion with the linearized coordinate  $r$ , so that we have

$$V(r) = ar^2 + br^4. \quad (23)$$

The continuity of mathematics and nature require that there exist eigenvalues  $E_v(a, b)$  for the potential (23) which are related by

$$\lim_{b \rightarrow 0} E_v(a, b) = E_v(a, 0) \quad (24)$$

with the eigenvalues  $E_v(a, 0) = h\omega(v + 1)$  of the harmonic oscillator (see eq. (14)). This is indeed true [30]. But the case is more complicated than it seems at first glance. Mathematically, we observe that  $E_v(1, b)$  as a complex function of  $b$  is not analytic at  $b = 0$  [30]. This implies that  $E_v(1, b)$  cannot have a convergent Taylor series, which represents it in any neighborhood of  $b = 0$ . Since the Taylor series is the basic feature of a perturbation approach, this means that our usual perturbation methods break down. That does not prevent the calculation of Taylor coefficients, and also does not eliminate the possibility that the resulting formal Taylor series converges, but not to the function  $E_v(1, b)$ ! Thus, the physical problem requires choosing other mathematical means to obtain convergent and realistic approximations. The WKB approximation has been tried [28]. The Padé diagonal approximants also converge better than the Taylor series. There are papers dealing with this problem from a mathematical point of view [31].

Note that in the pure quartic case  $r^4$  we still can obtain an analytical expression for the classical turning points by complete elliptic integrals [32], which is not possible in the general case  $r^m$ . Only for some special combinations of the constants  $a, b$ , and  $c$  in

$$V(r) = ar^2 + br^4 + cr^6 \quad (25)$$

do quasi-polynomial solutions still exist [33].

In spite of the mathematical problems outlined here, it has been conventional practice when  $b \ll a$  to try to understand the shift in the  $l$ -levels due to anharmonicity by the coefficients of the perturbation theory formulas [34]. As mentioned above, this can be dangerous. The resulting first correction to the energy is a term in  $l^2$ ,

$$E_{vl} = h\omega(v + 1) + g_{22}l^2, \quad (26)$$

which depends, insofar as we ignore influences of the two stretching modes in a rigid bender model, on coefficient  $b$  as

$$g_{22} = -b/2. \quad (27)$$

Thus, in contrast to the effects of the former potential of eq. (15), for  $b > 0$  we find now a downward shift of energy levels as  $l$  increases.

The large majority of linear molecules are well described at low excitation by a quadratic potential with only a small anharmonic contribution in one of the two categories discussed above. Covalently bonded molecules may be expected to fall into the category of case ii, while ionically bonded molecules show anharmonicity as in case i. The lifting of the  $l$ -degeneracy and its direction are the most obvious effects of either form of bending anharmonicity.

Spectroscopic data in reasonable rigid linear triatomic molecules, including covalently bonded species such as HCN [35], show that the energy levels usually go up with  $l$ . In the extended formula [2], including stretching effects, we find

$$g_{22} = -k_{2222}/48 + \frac{1}{16} \sum_{s=1,3} k_{s22}^2 \omega_s / (\omega_s^2 - 4\omega_2^2), \quad (28)$$

where  $k_{2222} = 24b$  and the  $k_{s22}$  are stretch–bend interaction constants in the expansion of the potential. Thus (a) either the stretch–bend interaction sum on the right hand side wins the competition over the quartic bending anharmonicity, or (b) the “Gaussian” limit is of more relevance than the “hinge” limit for these molecules, or (c) the observed  $g_{22}$  is dominated by the effect mentioned above, in which the degeneracy is lifted by the curvilinear nature and angular dependence of the reduced mass of the bending coordinate, or (d) the perturbative approach to the quartic potential is questionable. Points (a) and (b) are related, and constitute a challenging region of study in molecular physics which leads to the study of highly excited states.

#### 4. The quasilinear case

The term *quasilinear* is an empirical distinction meaning that the pattern of the energy levels of such a molecule resemble neither those of a linear nor those of a bent limiting case. Mathematically, this situation arises when the bending potential function is almost flat-bottomed (as with a nearly pure quartic potential), or the linear configuration corresponds to a local maximum on the PES (saddle point of index 2) [3] which lies near the ground state or the lowest excited vibrational levels, as illustrated in the PES which is the framework of fig. 10.

We represent this case by introducing a hump in the potential well  $V(\alpha, \phi) = V(\alpha)$ . The simplest form is again the potential function of eq. (22), but with a different restriction on the coefficients:

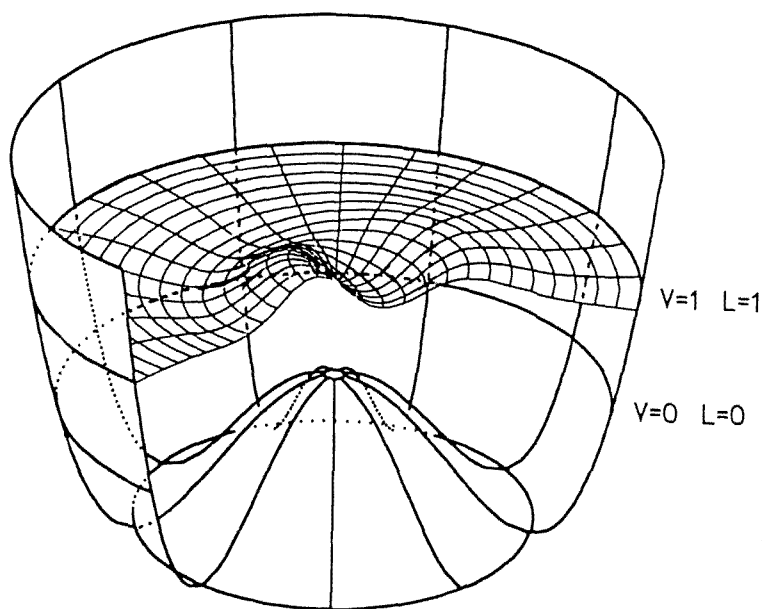


Fig. 10. Model PES of a quasilinear molecule, characterized by a hump, with real part of the wave function for  $v = 1$ . The radial coordinate is  $\alpha$ , and the coordinate of rotation of the figure is  $\phi$ .

$$V(\alpha) = a\alpha^2 + b\alpha^4 \quad \text{with } a \leq 0, b > 0. \quad (29)$$

This form has been used [36], for example, for describing HCNO and DCNO [37] (see refs. [4,31] for a compilation of other potential forms). Since the bending motion is of large amplitude, we maintain the actual bending angle  $\alpha$  as coordinate. There is a continuous range of potential functions and dynamic behavior from a harmonic linear molecule to a harmonic bent molecule, covered in the next section. In the range of cases that we call quasilinear, the lowest vibrational levels are close to, and are strongly affected by, the anharmonic bottom of the potential well. Viewed as a 2D function of both  $\alpha$  and  $\phi$ , this function has a circular minimum, as illustrated in the PES which is the framework of fig. 10; it does not depend on  $\phi$ . Both terms in eq. (29) are significant, indeed the walls of the potential well are dominated by the quartic term. A harmonic approximation now loses all usefulness. The accidental curvature of the potential function at the minimum bears no direct analytical relationship to the vibrational energy intervals.

As in the linear case, we consider two degrees of freedom: a bending and an angular coordinate with the two quantum numbers  $n$  and  $l$ . But now, the potential function does not have a minimum at the zero of the bending coordinate: on the contrary, it has a saddle point of index 2. In the classification of ref. [3] it is a *proper SP*, because it is characterized by the fact that the two included modes affect the same atoms or atomic groups.

Mathematically, this case is equivalent to the previous case described by eq.

(23), where  $a \geq 0$ , with all of its problems. Since now the quartic term dominates, rather than the quadratic one, however, these problems become acute. Spectroscopically, we generally observe a marked decrease of energy levels with increasing  $l$  for a given  $v$ . In this case the leading term in eq. (28) dominates clearly. Indeed, for a potential with a significant quartic contribution, the non-applicability of the perturbative treatment shows up in the fact that the  $g_{22}$  needed to represent the eigenvalues is not a constant, but changes as  $v$  increases [37].

A classic example is given by  $\text{SiH}_3\text{-O-SiH}_3$ , if we take it as a three-membered entity with two compact terminal  $\text{SiH}_3$  groups. This was actually the first molecule for which a quasilinear model was formulated [11,38,39]. The first three excited states, shown in fig. 11 with  $v = 1, 2$ , and 3, are "pure" rotational states in the circu-

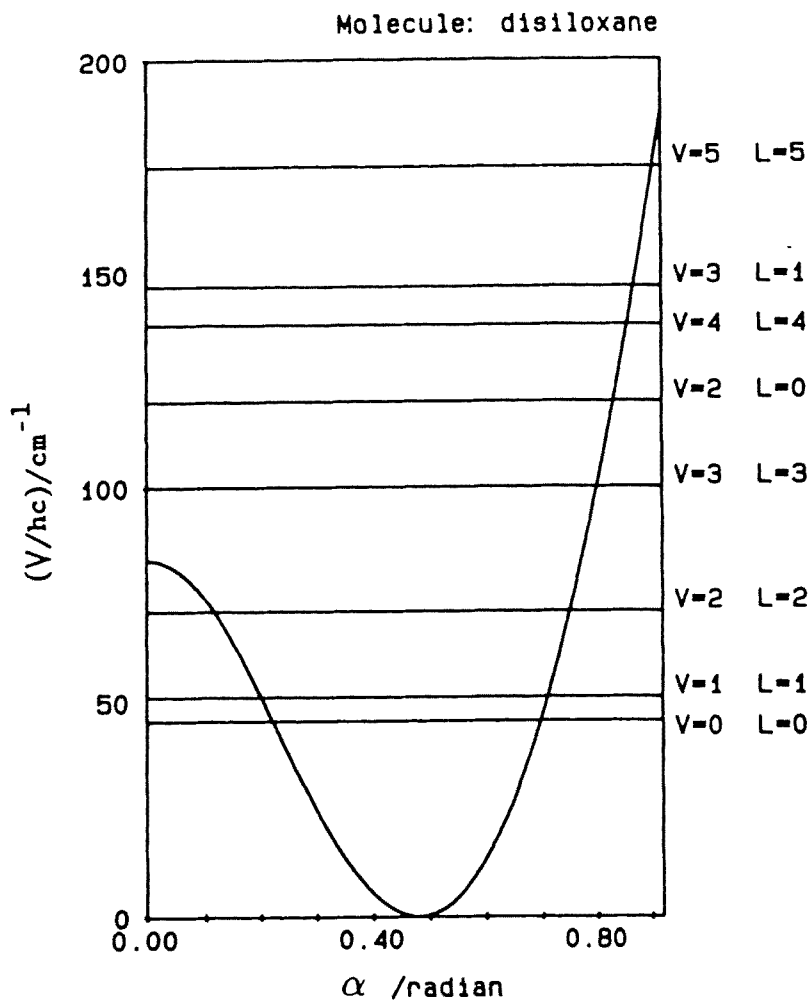


Fig. 11. 1D cut through the bending potential of the quasilinear molecule disiloxane. Included is the manifold of experimental energy levels  $(v, l)$  [38].



tain the 2D perspective, then the molecule finds no means to overcome the barrier to linearity at moderate excitation. The bending motion is restricted to an annular region of the potential surface. The oscillator can, as before, move in two directions: defined by  $x$  and  $y$  or  $\alpha$  and  $\phi$ . Here the angle  $\phi$  is a clearly defined Euler angle and rotational coordinate, since the plane of the atoms 1-2-3 in fig. 1 can now be unambiguously determined from the Eckart condition. The azimuthal motion thus corresponds now to a rotation with the quantum number  $K_a$ , the quantum number of angular momentum about the axis of least moment of inertia of the slightly asymmetric top which the bent molecule presents. This quantum number correlates directly with  $|l|$  in the linear and quasilinear cases, and describes pure rotation around the barrier. The orthogonal, bending coordinate  $\alpha$  delineates now a 1D-vibration across the well. So we arrive at the model of a harmonic oscillator (for bending) and rigid rotator. The hump can be interpreted as a local symmetry-breaking element of the former  $C_\infty$  potential, and is thus the reason for the applicability of all of the Eckart conditions in the bent case. Since  $r$  does not approach zero, no singularity in an effective potential over a "feasible" range of  $r$  emerges, the term  $l^2/r^2$  is well approximated using the constant value  $r_e$ , and thus, the coupling between bending and rotation in eq. (10) is nearly removed. As implied above by the use of the Eckart conditions, we now have a valid separation of variables, and the two vibrational degrees of freedom with which we started are reduced to a 1D vibration and one degree of rotational freedom, as originally expressed in eq. (1). The vibrational quantum number  $n$  in the basis function  $\psi_{nl}(r)$  is the number of nodes in  $r$ , which corresponds directly to the conventional numbering  $v_{(\text{bend})}$  for a bent molecule, as shown in fig. 13. The relation between linear and bent molecule bending quantum numbers is [18,40]

$$v_{(\text{linear})} = 2n + |l| = 2v_{(\text{bend})} + K \quad (30)$$

and it summarizes the continuity in the range of cases, from linear to bent, explored here.

A correlation between the two limiting cases is exhibited by rovibrational spectra across the full range of quasilinearity. A parameter to quantify molecular quasilinearity through the range where there is no closed expression for the energy levels was defined by Yamada and Winnewisser [41]. It is derived from the spacing pattern of the energy levels (measured or calculated) and is given by

$$\gamma = \frac{E(\text{lowest state with } K, \text{ or } l, = 1) - E(v = l = 0)}{E(\text{lowest excited st. with } K, \text{ or } l, = 0) - E(v = l = 0)}. \quad (31)$$

For a typical (harmonic) linear molecule, such as  $\text{CO}_2$  for example, we have  $\gamma = V(0, 1^1, 0)/V(0, 2^0, 0) \approx 1/2$ . The corresponding levels of a strongly bent molecule, such as  $\text{SO}_2$ , are determined by a rotational constant  $A$  and a high bending vibrational frequency, so that  $\gamma \approx 0.01$ .

Only a few molecular species are found with  $\gamma$  values far from these two limits. Most molecules are either "linear" or "bent", and most bent molecules are found

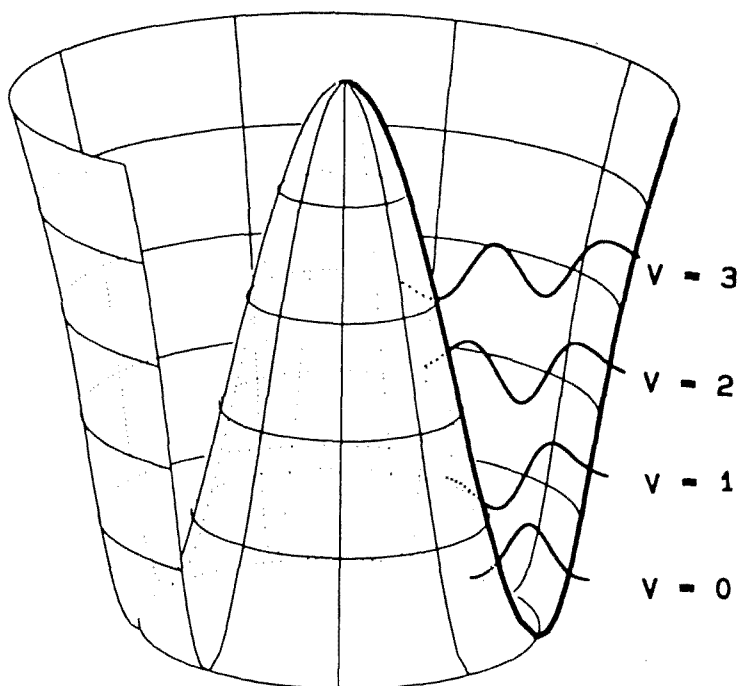


Fig. 13. Model PES of a bent molecule showing 1D wave functions of excited vibrational states, which are pure bending states. The cut through the surface indicated by the heavy line defines the 1D potential function.

to have a high barrier and equilibrium angles  $\alpha_{\text{eq}}$  in the range of  $50^\circ$ – $80^\circ$ . In these bent molecules, if we treat only excitations well below the barrier to linearity, we can again approximate the bending potential by a harmonic ansatz, now for a 1D potential. An extended mathematical discussion of 1D potential functions is found in a recent review [42].

On the other hand, if the height of the barrier to linearity of a bent triatomic molecule is lower than that of the outer wall of the bending potential (see fig. 13), any bent triatomic should show somewhere in its ladder of bending levels a transition to quasilinear behavior [40,43,44]. The change in behavior connects the two initially distinct degrees of freedom, the rotation about the  $a$  axis with rotational constant  $A$ , and the bending vibration. The rotational constant  $A$  in a bent molecule is defined by the interval between  $K = 0$  and 1. The change to quasilinearity is indicated by a very non-linear increase of the intervals defining the corresponding rotational constants  $A_v$ , in the ladder of bending vibrationally excited states  $v$ . The constants  $A_v$  change by one or two powers of ten and finally reach the vibrational frequency of the degenerate bending mode, in the 2D quasilinear situation. This transition is the result of a drastic increase of the  $l^2/r^2$  term in eq. (11). One candi-

date for this behavior is the intensively studied water molecule  $\text{H}_2\text{O}$  [45,46]. We cannot, of course, at high excitation, fully neglect the stretching modes. However, a highly excited  $\text{H}_2\text{O}$  molecule conquers even an energy barrier of about  $11000\text{ cm}^{-1}$ , and it continues to present riddles to the spectroscopist.

Occasionally the barrier in triatomic bent molecules has been described as an “inversion” barrier [47]. Inversion is generally accepted as meaning a distortion to an equivalent configuration that not only represents an inversion of coordinates but, more important, cannot be reached by a rotational operation, and which therefore introduces a doubling of all levels. In this sense there is no inversion in a triatomic molecule.

The T-shaped van der Waals molecules such as  $\text{Ar-N}_2$  [48] present the phenomenon of internal rotation of a strongly bound pair relative to the third atom. In such a case the barrier at the linear structure  $\alpha = 0$  has the same height as the outer wall, and our picture defined in the coordinates  $(\alpha, \phi)$  becomes inadequate. The outer threshold in figs. 9, 10, or 13 would correspond to the “next” linear structure at  $\alpha = 2\pi$ , and the whole extent of the outer wall would represent one and the same structure of the molecule. An internal rotation of the  $\text{N}_2$  group could go in any direction straight across the outer wall of this figure, to return on the opposite side. Thus, our mode of visualization is not appropriate for such species. The more suitable coordinates are the distance between the loosely-bound atom and the center of mass of the strongly bound pair and the angle between this distance vector and the axis of the strongly bound pair [48,49].

## 7. Outlook

Already in the simple cases of nonlinear triatomic molecules we find a combination of different singular points of the 2D isotropic PES well – namely a proper saddle point of index 2 and a flat ring. Such PES landscapes determine the spectroscopy of the corresponding molecules. Together with a “weighting” due to the kinetic energy, they give us a classification in linear, quasilinear, and bent molecules.

If we imagine a linear triatomic group attached to a larger molecule structure, we find a distortion of the 2D PES isotropy, so that the 2D presentation becomes even more necessary. The real molecules  $\text{HCNO}$  [50] and  $\text{HNCO}$  exhibit a twofold symmetry of the quasilinear  $\text{HXY}$  group against the  $\text{XYZ}$  bending. The rotational symmetry of each bending mode is distorted from the cylindrical symmetry of all the cases discussed above to an elliptical, and thus twofold, symmetry by a displacement of the bending coordinate at the other end of the molecule. The lifting of degeneracy in Renner–Teller interactions is an analogous situation. A treatment of a twofold symmetric potential goes back to Garnier [51], which is still a separable and integrable potential, and which is the first stage of a hierarchy of more complicated potentials [52].



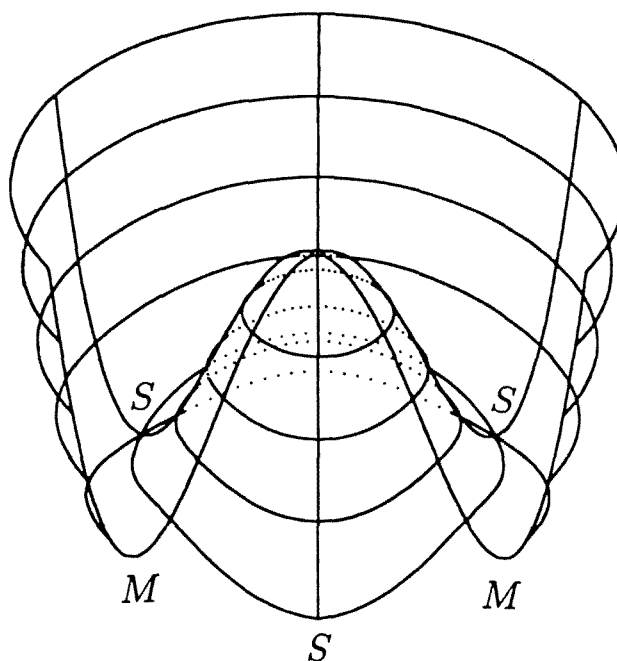


Fig. 14. Model PES with a minimum path around a saddle point of index 2 which has a three-fold rotational symmetry. This minimum path is now not flat, and the PES depends explicitly on  $\phi$ . The  $M$  are minima, and the  $S$  are ordinary saddle points.

The next category of distortion is illustrated by the case of  $\text{CH}_3\text{OH}$  [53], where the  $\text{CH}_3$ -umbrella imposes a threefold symmetry on the bending potential function of the  $\text{COH}$  group. As in the case of three-atomic species, there is a transition from a symmetric top with a 3-fold axis to an asymmetric top such as  $\text{CH}_3\text{OH}$ . For this example we redefine our molecule-fixed coordinates. We fix the  $z$  axis along the  $\text{CO}$  bond, and the  $x$  axis in the  $\text{OCH}$  plane of one of the hydrogens in the  $\text{CH}_3$  group. The PES for rotation of the  $\text{OH}$  group around the  $z$  axis then has the form illustrated in the model potential of fig. 14. With this choice of axes, the  $x$  axis coincides with one of the saddle points  $S$ . Also depicted are two of the three minima  $M$ .

$\text{SiH}_3\text{NCO}$ , for example, has a quasilinear  $\text{SiNC}$  bending mode and indications of a weak 3-fold barrier have been obtained [19,54]. The topography rapidly becomes more complex.

### Acknowledgements

We thank P. Jensen, M. Winnewisser, H. Dachsels, C.W. Mathews and G. Duxbury for helpful discussions. WQ thanks the Gießen Laboratory of Prof. M. Winne-

wisser for the kind hospitality. This work was supported by funds from the Fonds der Chemischen Industrie and the Deutsche Forschungsgemeinschaft. WQ thanks the Fonds der Chemischen Industrie for a stipend.

## References

- [1] R.J. Bartlett (ed.), *Comparisons of Ab Initio Quantum Chemistry with Experiments for Small Molecules* (Reidel, Dordrecht, 1985);  
W.J. Hehre, L. Radom, P.v.R. Schleyer and J.A. Pople, *Ab Initio Molecular Orbital Theory* (Wiley, New York, 1986).
- [2] D. Papoušek and M.R. Aliev, *Molecular Vibrational Rotational Spectra* (Academia, Prague, 1982).
- [3] D. Heidrich and W. Quapp, *Theor. Chim. Acta* 70 (1986) 89.
- [4] B.P. Winnewisser, in: *Molecular Spectroscopy – Modern Research*, Vol. III, ed. K. Narahari Rao (Academic Press, Orlando, 1985) ch. 6.
- [5] J.T. Hougen, P.R. Bunker and J.W.C. Johns, *J. Mol. Spectrosc.* 34 (1970) 136.
- [6] P. Jensen, *Comput. Phys. Rep.* 1 (1983) 1.
- [7] J. Tennyson, *Comput. Phys. Rep.* 4 (1986) 1.
- [8] S. Carter and N.C. Handy, *Comput. Phys. Rep.* 5 (1986) 115.
- [9] Z. Bačić and J.C. Light, *J. Chem. Phys.* 85 (1986) 4594.
- [10] P. Jensen, *J. Mol. Spectrosc.* 128 (1988) 478.
- [11] W.R. Thorson and I. Nagakawa, *J. Chem. Phys.* 33 (1960) 994.
- [12] J.D. Louck and H.W. Galbraith, *Rev. Mod. Phys.* 48 (1976) 69.
- [13] H. Triebel, *Höhere Analysis* (Deutsch. Verl. Wiss., Berlin, 1972). A glance at the literature shows an annoying ambiguity in the index ( $n + l$ ) of the associated Laguerre polynomial  $L_{n+l}^l$ , which may result in a misunderstanding; cf. the next reference.
- [14] S.G. Lieb, W.L. Perry and J.W. Bevan, *J. Comput. Chem.* 5 (1984) 115.
- [15] L.D. Landau and E.M. Lifschitz, III, *Quantenmechanik* (Akademieverl., 6. Aufl., Berlin, 1979).
- [16] H. Goldstein, *Classical Mechanics* (Addison-Wesley, London, 1950) p. 338.
- [17] P.W. Atkins, *Molecular Quantum Mechanics*, 2nd. Ed. (Oxford, 1983) p. 315.
- [18] W.H. Shaffer, *Rev. Mod. Phys.* 16 (1944) 245.
- [19] J.A. Duckett, Dissertation, University of Reading (1976).
- [20] R. Wallace, *Chem. Phys.* 76 (1983) 421.
- [21] P. Jensen and J. Terhürne, Program FARBE (Four Atomic Rigid BEnders), private communication.
- [22] J.P. Leroy and R. Wallace, *J. Chem. Phys.* 89 (1985) 1928.
- [23] K. Endl and R. Endl, *Computergrafik 1* (Würfelverlag, Biebertal-Vetzberg, 1989).
- [24] N.C. Handy, *Mol. Phys.* 61 (1987) 207.
- [25] K. Yamada, *Z. Naturforsch.* a38 (1983) 821.
- [26] J.K.G. Watson, *J. Mol. Spectrosc.* 101 (1983) 83.
- [27] E.F. Pearson, B.P. Winnewisser and M.B. Trueblood, *Z. Naturforsch.* a31 (1976) 1259.
- [28] R.L. Redington, *Spectrochim. Acta* A23 (1967) 1863.
- [29] D.J. Nesbitt and R. Naamen, *J. Chem. Phys.* 91 (1989) 3801.
- [30] B. Simon, *Ann. Phys. (NY)* 58 (1970) 76.
- [31] B.L. Burrows, M. Cohen and T. Feldmann, *J. Phys.* A22 (1989) 1303, and refs. therein.
- [32] T.W. Chen, *Am. J. Phys.* 48 (1980) 292.
- [33] B. Leaute and G. Marcilhacy, *J. Phys.* A19 (1986) 3527.
- [34] H.H. Nielsen, *Rev. Mod. Phys.* 23 (1951) 90.

- [35] W. Quapp, *J. Mol. Spectrosc.* 125 (1987) 122.
- [36] P.R. Bunker, B.M. Landsberg and B.P. Winnewisser, *J. Mol. Spectrosc.* 74 (1979) 9.
- [37] M. Winnewisser and B.P. Winnewisser, *J. Mol. Spectrosc.* 41 (1972) 143.
- [38] J.R. Durig, M.F. Flanagan and V.F. Kalasinsky, *J. Chem. Phys.* 66 (1977) 2775.
- [39] J. Koput, *Chem. Phys.* 148 (1990) 299.
- [40] I. Boháček, D. Papoušek, Š. Pick and V. Špirko, *Chem. Phys. Lett.* 42 (1976) 395.
- [41] K. Yamada and M. Winnewisser, *Z. Naturforsch.* a31 (1976) 139.
- [42] C. Rossetti, *La Revista Nuo. Cim.* 12 (No. 8) (1989) 1.
- [43] G. Herzberg, *Electronic Spectra and Electronic Structure of Polyatomic Molecules*, Vol. III (Von Nostrand, New York, 1977);  
G. Herzberg and K.K. Innes, *Can. J. Phys.* 35 (1957) 842.
- [44] Ch. Jungen, K-E.J. Hallin and A.J. Merer, *Mol. Phys.* 40 (1980) 25.
- [45] Yu.S. Makushkin, O.N. Ulenikov and I.V. Levashkin, *J. Mol. Spectrosc.* 144 (1990) 1.
- [46] P. Jensen, *J. Mol. Spectrosc.* 133 (1989) 438.
- [47] R. Zahradník, Z. Havlas, B.A. Hess Jr. and P. Hobza, *Coll. Czech, Chem. Commun.* 55 (1990) 869.
- [48] G. Brocks, *J. Chem. Phys.* 88 (1988) 578.
- [49] P.R. Bunker and D.J. Howe, *J. Mol. Spectrosc.* 83 (1980) 288.
- [50] P. Jensen, *J. Mol. Spectrosc.* 101 (1983) 422.
- [51] R. Garnier, *Rend. Circolo Mat. Palermo* 43 (1919) 155.
- [52] S. Wojciechowski, in: *Systéms dynamiques nonlineares*, ed. P. Winternitz (Pesses de l'Universite de Montreal, 1985) p. 294.
- [53] R.M. Minyaeb, M.E. Klezkij and B.I. Minkin, *Zh. Org. Khem.* 25 (1989) 469.
- [54] L. Halonen and I.M. Mills, *J. Mol. Spectrosc.* 98 (1983) 484.